



## THEORETICAL STUDY ON THE ADDITION REACTION MECHANISM BETWEEN PROPADIENYLIDENE AND FORMALDEHYDE: AN ALTERNATIVE APPROACH TO THE FORMATION OF FURAN

Ying JING,<sup>a</sup> Hui LIU,<sup>b,c</sup> Yang YU,<sup>b,c</sup> Xiaojun TAN,<sup>c,\*</sup> Hailong WANG,<sup>c</sup> Fang WANG<sup>c</sup>,  
Xinglou DU<sup>c</sup> and Yungang CHEN<sup>c</sup>

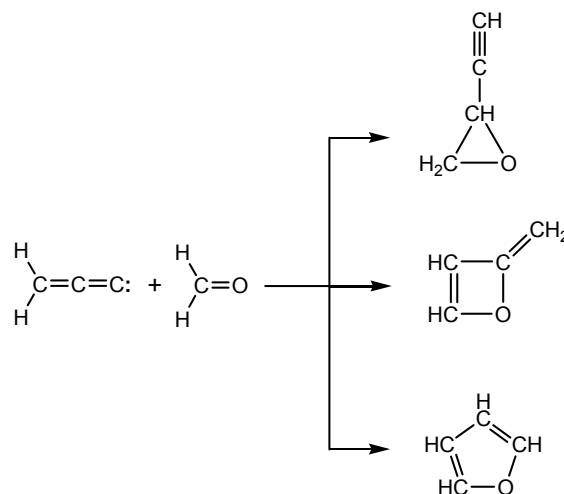
<sup>a</sup> The General Hospital of Jinan Military Command, Jinan, Shandong, 250031, People's Republic of China

<sup>b</sup> Shandong Academy of Medical Sciences, Jinan, Shandong, 250062, People's Republic of China

<sup>c</sup> College of Medical and Life Science, University of Jinan, Jinan, Shandong, 250022, People's Republic of China

Received April 17, 2013

The reaction mechanism between propadienylidene and formaldehyde has been systematically investigated employing the second-order Moller-Plesset perturbation theory (MP2) method to better understand the reactivity of propadienylidene with formaldehyde. Geometry optimization, vibrational analysis, and energy property for the involved stationary points on the potential energy surface have been calculated. One important initial intermediate characterized by three-atoms ring structure has been formed via a transition state firstly. After that, three different products possessing three-, four-, and five-atoms ring characters have been obtained through three reaction pathways. In the first reaction pathway, a three-atoms ring alkyne compound has been obtained. As for the second reaction pathway, it is the formation of the four-atoms ring conjugated diene compound. In the third reaction pathway, furan has been obtained finally, which is the most stable product in the available products thermodynamically.



### INTRODUCTION

Carbene can be defined as divalent carbon intermediates, where the carbene carbon is linked to two adjacent groups by covalent bonds and possesses two nonbonding electrons. It is well known that carbene plays an important role in organic chemistry, especially for the addition reaction with the C=C and C=O double bonds.<sup>1-3</sup> Therefore, the studies of carbene have attracted more attentions theoretically and experimentally. For example, carbene can be used to provide simple and direct synthesis for small-ring, highly

strained compounds, as well as those that are hard to synthesize through conventional ways.<sup>4</sup> The reactions between carbene or substituted carbenes and some small molecules have been studied theoretically by Lu *et al.*<sup>5-7</sup> Apeloig *et al.* extensively studied the mechanisms and stereoselectivity of carbene addition to olefin experimentally and theoretically.<sup>8,9</sup>

C<sub>3</sub>H<sub>2</sub> is a class of highly unsaturated carbenes, which is of great interest for the chemistry of carbon-rich gas-phase environments. As displayed in Scheme 1, three isomers have been located on its potential energy surface. Here, propynylidene is the only C<sub>3</sub>H<sub>2</sub> isomer with triplet electronic ground

\* Corresponding author: [chm\\_tanxj@ujn.edu.cn](mailto:chm_tanxj@ujn.edu.cn)

state and the propadienylidene and cyclopropenylidene are in singlet state.<sup>10-13</sup> Moreover, all of them can be interconverted by photolysis.<sup>14-16</sup> The structural characters, thermochemistry, and isomerization of  $C_3H_2$  carbenes have been investigated extensively.<sup>10,15,17-19</sup> It was found that the singlet cyclopropenylidene is the most stable isomer among the three species, which is lower in energy about 42-59 and 59-92 kJ/mol than that of the propadienylidene and propynylidene, respectively.<sup>20-28</sup> These highly reactive carbene molecules are fundamentally important not only within the context of organic chemistry, but also within the context of the chemistry of the interstellar medium.<sup>29,30</sup> Recently, the formation mechanism of the  $C_3H_2$  carbene has been proposed by Goulay *et al.* using tunable vacuum ultraviolet photoionization and time-resolved mass spectrometry.<sup>31</sup>

In the absence of experimental information, a theoretical investigation on the reaction between  $C_3H_2$  carbene and carbonyl compounds appears to be highly desirable and practical. Moreover, it has been reported that propadienylidene is the final product by the photolysis of cyclopropenylidene. Therefore, in the present study, the addition reaction mechanism between propadienylidene and formaldehyde has been systematically investigated employing the second-order Moller-Plesset perturbation theory (MP2) method so as to better understand the propadienylidene reactivity with unsaturated carbonyl compounds. As mentioned below, three different products characterized by 3-, 4-, and 5-atoms ring have been obtained via three different reaction pathways. The corresponding reaction mechanisms have been clarified detailedly. Hopefully, the present results not only can promote the progress of the relevant experiments, but also can provide insights into the reactivity of  $C_3H_2$  carbene with unsaturated carbonyl compounds containing double bonds as well as to enrich the available data for the relevant carbene chemistry.

## CALCULATION METHOD

The second-order Møller-Plesset perturbation theory (MP2) method<sup>32</sup> in combination with the 6-

311+G\* basis set has been employed to locate all the stationary points along the reaction pathways. Frequency analyses has been carried out to confirm the nature of the minima and transition states. Moreover, intrinsic reaction coordinate (IRC) calculations have also been performed to further validate the calculated transition states connecting reactants and products. Additionally, the relevant energy quantities, such as the reaction energies and barrier heights, have been corrected with the zero-point vibrational energy (ZPVE) corrections.

To further refine the calculated energy parameters, single point energy calculations have been performed at the CCSD(T)/6-311+G\* level of theory. As summarized in Table 1, both operations can give consistent results for the calculated reaction profile of the addition reaction. For the sake of simplicity, the energetic results at the MP2/6-311+G\* level have been mainly discussed below if not noted otherwise.

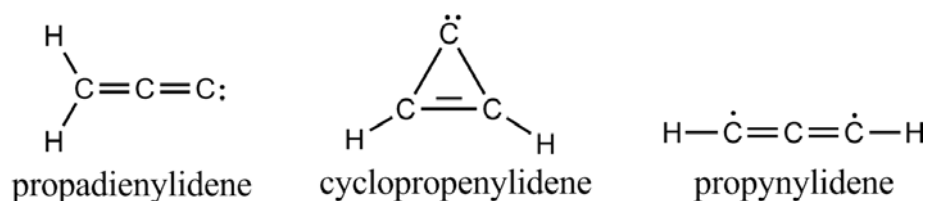
All the calculations have been performed using Gaussian 98 program.<sup>33</sup>

## RESULTS AND DISCUSSION

As displayed in Scheme 2, three possible reaction pathways involving the three products for the addition reaction between propadienylidene and formaldehyde have been proposed. Correspondingly, the calculated relative energies for the available stationary points have been summarized in Table 1.

*Reaction pathway (1): the formation of a three-atoms ring product (P1)*

The geometric parameters for the reactants, transition states (TS, TS1A and TS1B), intermediates (INT, INT1A), and product (P1) involved in the reaction pathway (1) are displayed in Fig. 1. Here, a three-atoms ring product P1 has been obtained in this pathway. The corresponding reaction profile is illustrated in Fig. 2.

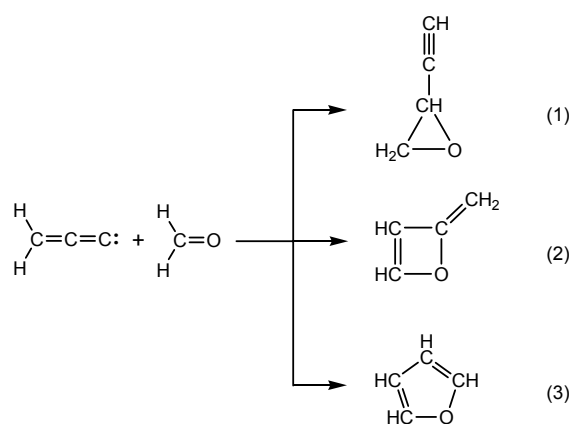


Scheme 1 – The three isomers of  $C_3H_2$

Table 1

The calculated relative energy (in kJ/mol) with respect to the isolated reactants <sup>a</sup>

Pathways	Relative Energies				
<b>Pathway (1)</b>	<b>TS</b> 12.4/7.9	<b>INT</b> -212.5/-203.2	<b>TS1A</b> 99.9/110.0	<b>INT1A</b> 1.1/1.4	<b>TS1B</b> 132.3/144.7
	<b>P1</b> -262.1/-238.4				
<b>Pathway (2)</b>	<b>TS2A</b> 49.7/64.5	<b>INT2A</b> -44.0/-56.1	<b>TS2B</b> -11.4/-8.3	<b>P2</b> -299.0/-289.2	
<b>Pathway (3)</b>	<b>TS3A</b> 23.0/40.8	<b>INT3A</b> -134.8/-148.3	<b>TS3B</b> 8.7/14.9	<b>INT3B</b> -18.1/-3.5	<b>TS3C</b> 107.7/133.4
	<b>INT3C</b> -29.0/-15.0	<b>TS3D</b> 6.9/13.9	<b>INT3D</b> -49.0/-52.0	<b>TS3E</b> 79.9/88.3	<b>INT3E</b> -193.3/-187.7
	<b>TS3F</b> 71.4/99.2	<b>INT3F</b> -223.7/-226.2	<b>TS3G</b> -178.6/-165.5	<b>P3</b> -487.4/-467.8	

<sup>a</sup> The data after the slash refer to the results at the CCSD(T)//MP2/6-311+G\* level of theory.

Scheme 2 – The proposed reaction pathways for the addition reaction.

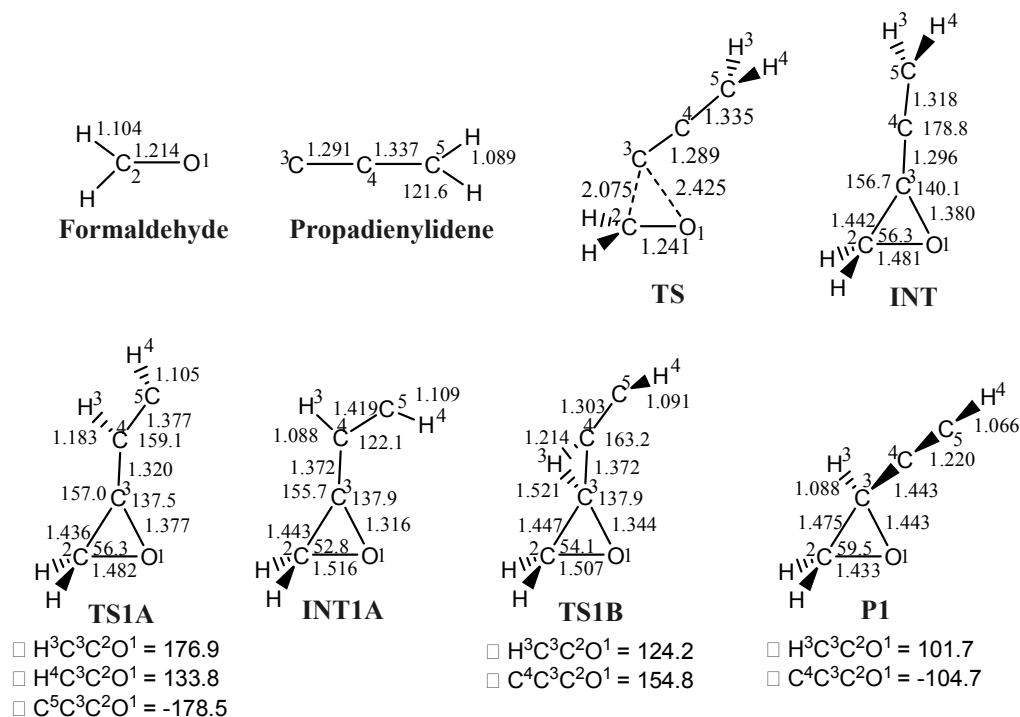


Fig. 1 – Optimized structures of the reactants (propadienylidene and formaldehyde), transition states (TS), intermediates (INT), and products (P) in the reaction pathway (1) at the MP2/6-311+G\* level of theory, where the bond length and bond angle are in angstrom and degree, respectively.

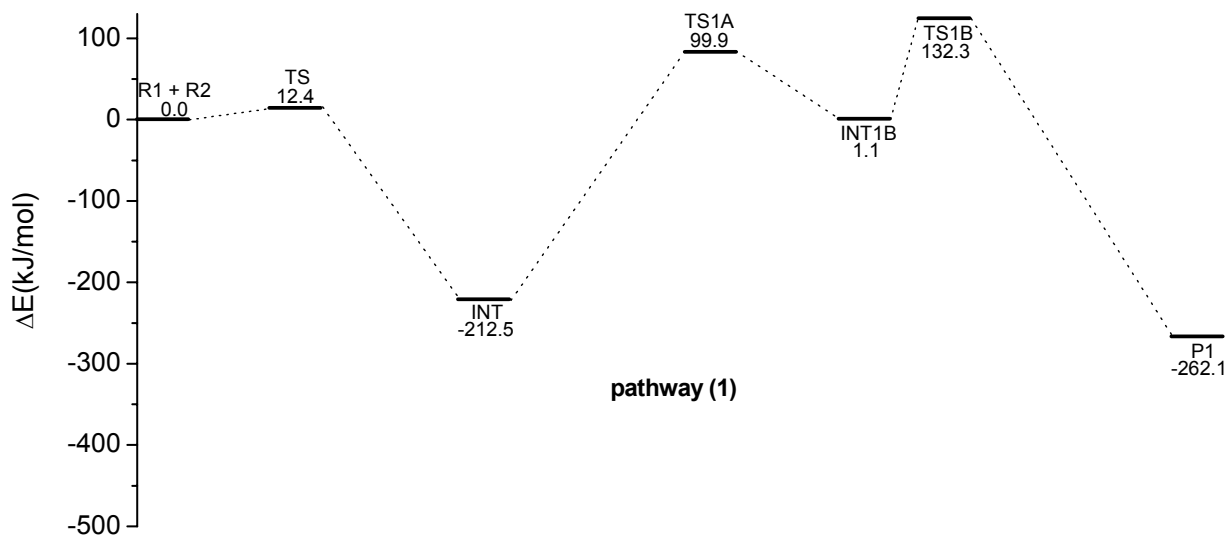


Fig. 2 – Reaction profile for the addition reaction pathways (1) between propadienylidene and formaldehyde at the MP2/6-311+G\* level of theory.

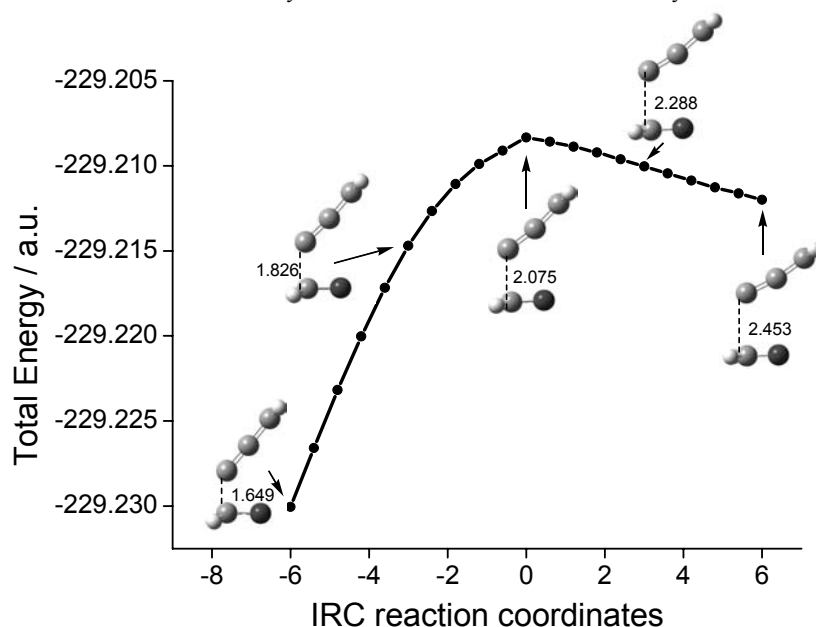


Fig. 3 – IRC of TS and geometry evolution.

The first intermediate INT occurs along the pathway (1), (2), and (3) via a rather small barrier of 12.4 kJ/mol. TS has a  $C_s$  symmetry, propadienylidene and the C=O group of formaldehyde being in the same plane. As shown in Fig. 1, the distances from  $C^3$  to  $O^1$  and  $C^2$  in TS are 2.425 and 2.075 Å, and the bond lengths of  $C^3C^4$ ,  $C^4C^5$ , and  $O^1C^2$  are only slightly changed (1.289 vs 1.291, 1.335 vs 1.337, 1.241 vs 1.214 Å) as compared with the reactants. The smoothness of the full IRC shown in Fig. 3 further indicates that TS connects reactants and the three-atoms ring intermediate INT. The IRC trajectory also shows that  $C_s$  symmetry is maintained along the forming of INT.

According to the geometric evolution along the process of forming INT and frontier molecular orbital (MO) analysis as illustrated in Fig. 4, orbital interactions are supposed as follows for the formation of INT. The unoccupied  $p$  orbital (main component of LUMO) of the  $C^3$  end of propadienylidene overlaps with the  $\sigma$  electron highly polarized at the  $O^1$  end of formaldehyde, while the lone pair  $\sigma$  electrons of propadienylidene overlap with the antibonding  $\pi^*$  (LUMO) orbital mainly located at  $C^2$  of formaldehyde, consequently forming  $\pi \rightarrow p$  of  $O^1-C^3$  and  $\sigma \rightarrow \pi^*$  of  $C^3-C^2$  donor-acceptor bonds, which change the reactants into the intermediate INT via the transition state TS.

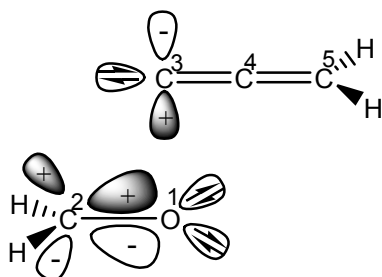


Fig. 4 – Frontier molecular orbital (MO) symmetry-adaption of  $\text{CH}_2\text{CC}:$  and  $\text{HCHO}$ .

As displayed in Fig. 1, in INT, the  $\text{C}^4$  adopts  $sp$  hybridization and the C-C bond lengths are 1.318 ( $\text{C}^4\text{-C}^5$ ) and 1.296 ( $\text{C}^3\text{-C}^4$ ) Å, which is somewhere between the general  $\text{C}=\text{C}$  double bond (about 1.33 Å) and  $\text{C}\equiv\text{C}$  triple bond (about 1.20 Å), respectively. These bond lengths suggest that INT possesses the feature of a normal allen, which can be further isomerized to an alkyne structure. Therefore, the second step of the pathway (1) is the hydrogen atom transfer of INT from the  $\text{C}^5$  to  $\text{C}^4$  atom via TS1A, resulting in the formation of the intermediate INT1A.

In INT1A, the  $\text{C}^4$  adopts  $sp^2$  hybridization and the  $\text{C}^4\text{-C}^5$  and  $\text{C}^3\text{-C}^4$  bonds have been changed to the single and double bond, respectively. As for the

$\text{C}^5$  atom, it has a pair of lone electrons, making the INT1A exhibit the carbene characters. In other words, INT1A is unstable and can rearrange to a more stable structure.

By shifting the  $\text{H}^3$  atom on the  $\text{C}^4$  to adjacent  $\text{C}^3$ , INT1A can be converted to P1 via TS1B. Here, P1 is the most stable structure along the pathway (1). Obviously, in P1, the  $\text{C}^3$  is  $sp^3$  hybridization and both the  $\text{C}^4$  and  $\text{C}^5$  are  $sp$  hybridization. Therefore, the bond between the  $\text{C}^4$  and  $\text{C}^5$  is a triple bond (1.220 Å), which is rather shorter than that of the bond between  $\text{C}^3$  and  $\text{C}^4$  (1.443 Å).

For the pathway (1), the three steps need to surmount transition state. The corresponding barrier of the three steps are 12.4, 312.4 and 131.2 kJ/mol, respectively. Therefore, the second step is the rate-determining step along the pathway (1).

*Reaction pathway (2): the formation of a four-atoms ring product (P2)*

The geometric parameters for the stationary points in the reaction pathway (2) are given in Fig. 5, where a four-atoms ring product (P2) has been generated in this pathway. The corresponding reaction profile is illustrated in Fig. 6.

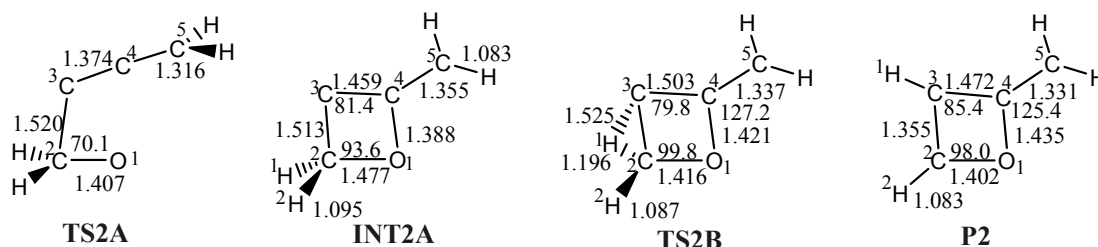


Fig. 5 – Optimized structures of the transition state (TS), intermediates (INT), and product (P) in the reaction pathway (2) at the MP2/6-311+G\* level of theory, where the bond length and bond angle are in angstrom and degree, respectively.

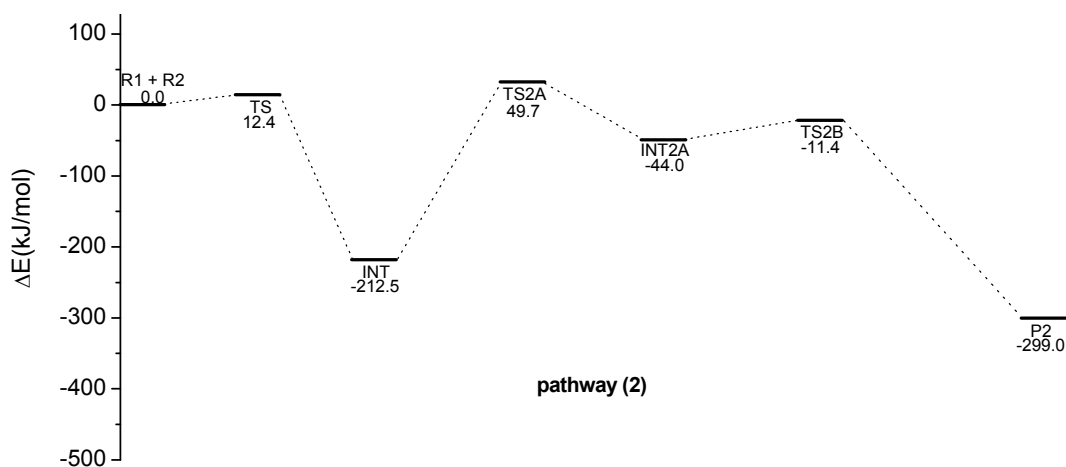


Fig. 6 – Reaction profile for the addition reaction pathways (2) between propadienylidene and formaldehyde at the MP2/6-311+G\* level of theory.

Similar to the reaction pathway (1), a common intermediate (INT) has been formed firstly. For the existence of tension in three-atoms ring, the second step of the pathway (2) is that O<sup>1</sup>-C<sup>3</sup> bond opened to form an intermediate INT2A via TS2A, where the barrier is 262.2 kJ/mol.

Note that there are a pair of lone electrons on the C<sup>3</sup> of INT2A. Therefore, the third step of the pathway (2) is that one H atom on the C<sup>2</sup> of INT2A is transferred to the C<sup>3</sup> to form a more stable structure P2 via TS2B, where the barrier is 32.6 kJ/mol. Based on the analysis of the imaginary frequency and the calculation of the IRC, it can be proved that TS2B connected the INT2A and P2 indeed.

For the structure of P2, the bond length of the C<sup>2</sup>-C<sup>3</sup> and C<sup>4</sup>-C<sup>5</sup> is 1.355 and 1.331 Å, respectively, which is slightly longer than that of the normal C=C double bond. At the same time, the bond length of the C<sup>3</sup>-C<sup>4</sup> is 1.472 Å, which is slightly shorter than that of the normal C-C single

bond. Moreover, further energy analyses suggest that P2 is lower about 299.0 kJ/mol than those of the reactants. From the calculated bond length and the stability, one can say that P2 is a stable conjugated diene and it is the ultima product of the pathway (2).

#### Reaction pathway (3): the formation of furan (P3)

The geometric parameters for the stationary points in the reaction pathways (3) are given in Fig. 7. The corresponding reaction profile is illustrated in Fig. 8. As illustrated in Fig. 7, a five-atoms ring product furan (P3) has been produced.

In command with the pathway(2) and (3), the first step of the pathway (3) is forming the initial intermediate INT. As mentioned above, there is an unstabled three-atoms ring in the INT. The second step of the pathway (3) is that C<sup>2</sup>-C<sup>3</sup> bond opened to form an intermediate INT3A via TS3A, where the barrier is 235.5 kJ/mol.

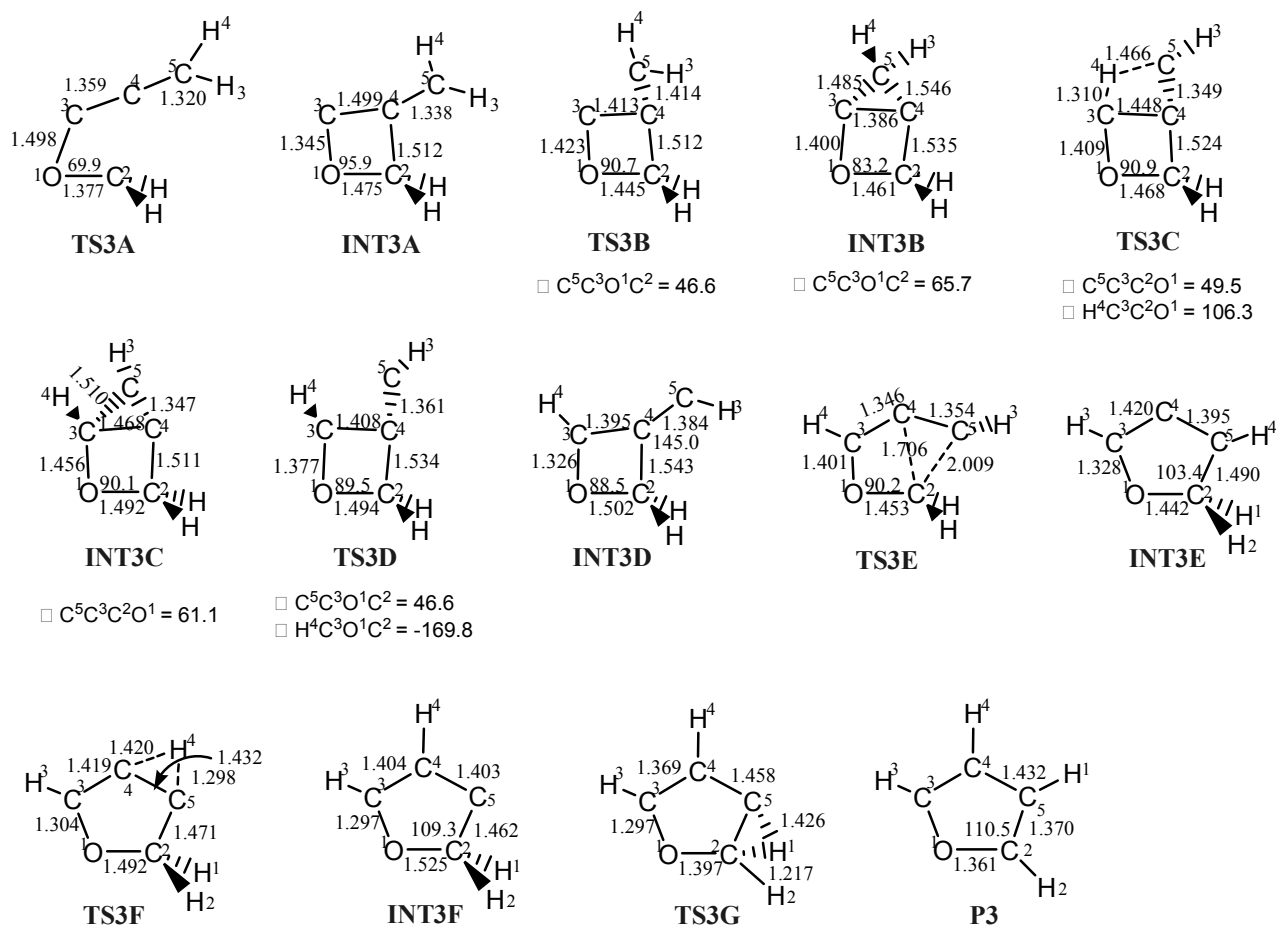


Fig. 7 – Optimized structures of the initial reaction complexes (RC), transition states (TS), intermediates (INT), and product (P) in the reaction pathways (3R) and (3L) at the MP2/6-311+G\* level of theory, where the bond length and bond angle are in angstrom and degree, respectively.

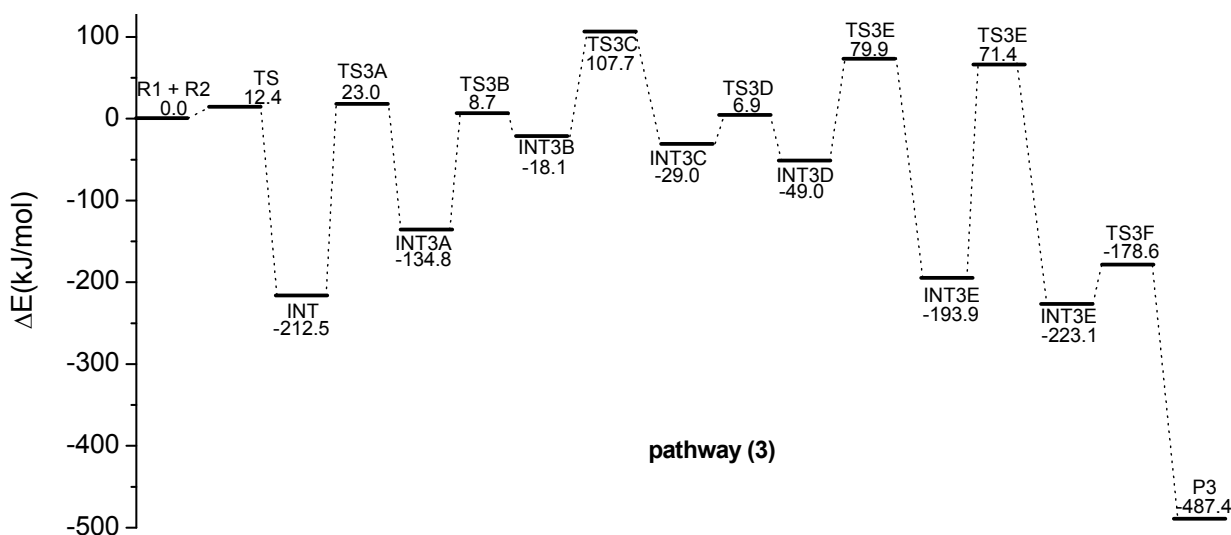


Fig. 8 – Reaction profile for the addition reaction pathways (3) between propadienylidene and formaldehyde at the MP2/6-311+G\* level of theory.

Relative to the three-atoms ring structure of INT, INT3A has four-atoms ring structure. However, because of existing of a pair of lone electrons on C<sup>3</sup>, INT3A is high 77.7 kJ/mol than that of INT.

By means of the torsion of the C<sup>5</sup>, the lone electrons of the C<sup>3</sup> of INT3A can form one  $\sigma$  bond and one  $\pi$  bond with the C<sup>5</sup> and C<sup>4</sup>, respectively. Therefore, the third step of the reaction pathway (3) is the formation of the INT3B from INT3A via TS3B.

After that, a hydrogen atom migration reaction occurs in the fourth step, resulting in the formation of the INT3C via TS3C. In this step, the  $\pi$  bond between the C<sup>3</sup> and C<sup>4</sup> is unfolded, which can produce a lone electron on the C<sup>3</sup> and C<sup>4</sup>, respectively. The lone electron on the C<sup>3</sup> interacts with the H<sup>4</sup> to form a C<sup>3</sup>-H<sup>4</sup>  $\sigma$  bond. Meanwhile, the other lone electron on the C<sup>4</sup> interacts with the C<sup>5</sup> to form a C<sup>4</sup>-C<sup>5</sup>  $\pi$  bond. Therefore, the C<sup>4</sup>-C<sup>5</sup> single bond in INT3B has been changed to a double bond in INT3C. Note that INT3C is an endocyclic compound, where the C<sup>3</sup>-C<sup>4</sup> bond has been shared by the three-atoms ring involving the C<sup>3</sup>, C<sup>4</sup>, C<sup>5</sup> and the four-atoms ring formed among the O<sup>1</sup>, C<sup>2</sup>, C<sup>3</sup>, and C<sup>4</sup>, respectively. Expectedly, the three-atoms ring in INT3C should be easily destroyed due to its high strain.

Due to the weak single bond between the C<sup>3</sup> and C<sup>5</sup> relative to that of the double bond between the C<sup>4</sup> and C<sup>5</sup> in INT3C, ring-opening reaction occurs via the rupture of the C<sup>3</sup>-C<sup>5</sup> bond. After that, a single electron is generated on the C<sup>3</sup>, which can form a  $\pi$  bond with the electron on the C<sup>4</sup>. Therefore, in the fifth step, INT3D is formed via TS3D. The C<sup>3</sup>-C<sup>4</sup> bond length in INT3D is 1.395 Å,

which is the typical length of the C=C double bond. At the same time, INT3D also possesses the carbene characters because of its lone electrons on the C<sup>5</sup> atom, implying that it can be further transformed to a more stable structure.

As expected, the sixth step of the pathway (3) is the formation of the INT3E from INT3D via TS3E. As displayed in Fig. 6, in TS3E, the distance between the C<sup>2</sup> and C<sup>4</sup> has been elongated by 0.163 Å compared with that in INT3D, denoting the break of the C<sup>2</sup>-C<sup>4</sup> bond. At the same time, the distance between the C<sup>2</sup> and C<sup>5</sup> is decreased to 2.009 Å, denoting the forming of a new bond between them.

Subsequently, in the seventh step of the pathway (3), INT3E can isomerize to a more stable structure via the hydrogen atom transfer. Namely, the H<sup>4</sup> atom on the C<sup>5</sup> of it can be transferred to the C<sup>4</sup> atom to form INT3F. Similar to INT3E, INT3F is also characterized by a five-atoms ring and has a pair of lone electrons on C<sup>5</sup> atom. However, the O<sup>1</sup>C<sup>2</sup>C<sup>5</sup> angle associated with the five-atoms ring in the INT3E and INT3F is 103.4 and 109.3°, respectively. Therefore, the ring strain in the INT3F is lower than that of the INT3E. As a result, INT3F is more stable about 29.2 kJ/mol than INT3E as displayed in Fig. 8.

Finally, one of the H atoms on the C<sup>2</sup> of INT3F, such as H<sup>1</sup> atom here, can be transferred to the adjacent C<sup>5</sup> to form the most stable product furan via TS3G in the eighth step. This is a simple hydrogen atom transfer reaction, where the corresponding barrier is 44.6 kJ/mol. After that, for the quondam lone electrons on the C<sup>5</sup> of INT3F, one of them will form a C<sup>5</sup>-H<sup>1</sup>  $\sigma$  bond and the other

one will form a C<sup>5</sup>-C<sup>2</sup>  $\pi$  bond. Accordingly, the bond length of the C<sup>5</sup>-C<sup>2</sup> has been shortened from 1.462 (in INT3F) to 1.370 Å (in P3). Here, it should be noted that furan has been stabilized by about 487.4 kJ/mol relative to the initial reactants.

In summary, the barrier height of the eight steps along pathway (3) is 12.4, 235.5, 143.5, 125.8, 35.9, 128.9, 265.3, and 44.6 kJ/mol, respectively. Therefore, the seventh step is the rate-determining step along the pathway (3).

#### Comparisons of the three reaction pathways

As mentioned above, three-, four-, and five-atoms ring products can be produced between propadienylidene and formaldehyde through different reaction pathways. The barrier height of the rate-determining step in the reaction pathways (1), (2), and (3) is 312.4, 262.2, and 265.3 kJ/mol, respectively. Therefore, the reaction pathway (2) is the most favorable channel from the kinetic viewpoint. On the other hand, the corresponding three products P1, P2, and P3 have been stabilized by about 262.1, 299.0, and 487.4 kJ/mol relative to the reactants, respectively. Therefore, the most favorable product P3 (furan) should be confirmed, implying that the reaction pathway (3) is also favorable channel from the thermodynamical viewpoint. The pathway (3) can provide an alternative approach to the formation of furan. Certainly, the final product should be controlled by the nature of the reaction, *i.e.*, the whole addition process is whether the kinetically controlled or the thermodynamically controlled reaction. To clarify this point, more relevant experiments are highly desirable in the near future.

### CONCLUSIONS

In this study, the reaction mechanism between propadienylidene and formaldehyde has been systematically investigated employing the MP2/6-311+G\* levels of theory and correction energy at CCSD(T)//MP2/6-311+G\*. It was found that an initial reaction intermediate has been formed firstly. After that, three different products characterized by the three-, four-, and five-atoms ring have been obtained through different pathways. The barrier of the rate-determining step of the three reaction pathways is 312.4, 262.2, and 265.3 kJ/mol, respectively. On the other hand, the corresponding products P1, P2, and P3 have been stabilized by 262.1, 299.0, and 487.4 kJ/mol relative to the reactants, respectively. Therefore,

the second reaction pathway is the most favorable reaction to occur kinetically, which is a diffusion-controlled reaction. However, the high stability of P3 among the available products suggest that the corresponding reaction pathway is also a favorable process thermodynamically, providing an alternative approach to the formation of the furan.

*Acknowledgments:* This work is supported by Project of Shandong Province Higher Educations Science and Technology Program (J13LM06, J10LF03, J13LM53), National Undergraduate Training Programs for Innovation and Entrepreneurship (201210427010), and SRT of University of Jinan.

### REFERENCES

1. M. Mitani, Y. Kobanashi and K. Koyama, *J. Chem. Soc. Perkin Trans. I*, **1995**, 6, 653-655.
2. M. Garcia, C. D. Campo and E. F. Llama, *J. Chem. Soc. Perkin Trans. I*, **1995**, 13, 1771-1773.
3. R. R. Kostikov, A. F. Khlebnikov and V. Y. Bespalov, *J. Phys. Org. Chem.*, **1993**, 6, 83-84.
4. Y. Wang, H. R. Li, C. M. Wang, Y. J. Xu and S. J. Han, *Acta Phys-Chim. Sin.*, **2004**, 20, 1339-1344.
5. P. J. Stang, *Acc. Chem. Res.*, **1982**, 15, 348-354.
6. X. H. Lu and Y. X. Wang, *J. Phys. Chem. A*, **2003**, 107, 7885-7890.
7. X. H. Lu and Y. X. Wang, *J. Mole. Struct. (THEOCHEM)*, **2004**, 686, 207-211.
8. Y. Apeloig, M. Karni and P. J. Stang, *J. Am. Chem. Soc.*, **1983**, 105, 4781-4792.
9. D. P. Fox, P. J. Stang, Y. Apeloig and M. Karni, *J. Am. Chem. Soc.*, **1986**, 108, 750-756.
10. R. Herges and A. Mebel, *J. Am. Chem. Soc.*, **1994**, 116, 8229-8237.
11. G. Maier, H. P. Reisenauer, W. Schwab, P. Carsky, B. A. Hess and L. J. Schaad, *J. Am. Chem. Soc.*, **1986**, 108, 5183-5188.
12. R. A. Seburg, J. T. DePinto, E. V. Patterson and R. McMahon, *J. Am. Chem. Soc.*, **1995**, 117, 835-836.
13. T. MacAllister and A. Nicholson, *J. Chem. Soc. Faraday Trans. 1*, **1981**, 77, 821-825.
14. R. A. Seburg and R. MacMahon, *Angew. Chem. Int. Ed. Engl.*, **1995**, 34, 2009-2012.
15. R. A. Seburg, E. V. Patterson, J. F. Stanton and R. J. McMahon, *J. Am. Chem. Soc.*, **1997**, 119, 5847-5856.
16. G. Maier, H. P. Reisenauer, W. Schwab, P. Carsky, V. Spirko, B. A. Hess and L. J. Schaad, *J. Chem. Phys.*, **1989**, 91, 4763-4774.
17. V. Juana, E. H. Michael, G. Jurgen and F. S. John, *J. Phys. Chem. A*, **2009**, 113, 12447-12453.
18. C. A. Taatjes, S. J. Klippenstein, N. Hansen, J. A. Miller, T. A. Cool, J. Wang, M. E. Law and P. R. Westmoreland, *Phys. Chem. Chem. Phys.* **2005**, 7, 806-813.
19. K. C. Lau and C. Y. Ng, *Chin. J. Chem. Phys.*, **2006**, 19, 29-38.
20. R. Gleiter and R. Hoffmann, *J. Am. Chem. Soc.*, **1968**, 90, 5457-5460.
21. R. Shepard, A. Banerjee and J. Simons, *J. Am. Chem. Soc.*, **1979**, 101, 6174-6178.



22. T. J. Lee, A. Bunge and H. F. Schaefer, *J. Am. Chem. Soc.*, **1985**, *107*, 137-142.
23. J. A. Montgomery, J. W. Ochterski and G. A. Petersson, *J. Chem. Phys.*, **1994**, *101*, 5900-5909.
24. W. J. Hehre, J. A. Pople and W. A. Lathan, *J. Am. Chem. Soc.*, **1976**, *98*, 4378-4383.
25. V. Jonas, M. Bohme and G. Frenking, *J. Phys. Chem.*, **1992**, *96*, 1640-1648.
26. J. Takahashi and K. Yamashita, *J. Chem. Phys.*, **1996**, *104*, 6613-6627.
27. Q. Fan and G. V. Pfeiffer, *Chem. Phys. Lett.*, **1989**, *162*, 472-478.
28. S. P. Walch, *J. Chem. Phys.*, **1995**, *103*, 7064-7071.
29. E. Herbst, *Angew. Chem. Int. Ed. Engl.*, **1990**, *29*, 595-599.
30. P. Thaddeus, C. A. Gottlieb, R. Mollaaghababa and M. V. Jan, *J. Chem. Soc. Faraday Trans.*, **1993**, *89*, 2125-2129.
31. G. Fabien, J. T. Adam, M. Giovanni, *J. Am. Chem. Soc.*, **2009**, *131*, 993-1005.
32. M. Head-Gordon, J. A. Pople, and M. J. Frisch, *Chem. Phys. Lett.*, **1988**, *153*, 503-506.
33. M. J. Frisch, G. W. Trucks, H. B. Schlegel, G. E. Scuseria, M. A. Robb, J. R. Cheeseman, V. G. Zakrzewski, J. A. Montgomery, R. E. Stratmann, Jr., J. C. Burant, S. Dapprich, J. M. Millam, A. D. Daniels, K. N. Kudin, M. C. Strain, O. Farkas, J. Tomasi, V. Barone, M. Cossi, R. Cammi, B. Mennucci, C. Pomelli, C. Adamo, S. Clifford, J. Ochterski, G. A. Petersson, P. Y. Ayala, Q. Cui, K. Morokuma, D. K. Malick, A. D. Rabuck, K. Raghavachari, J. B. Foresman, J. Cioslowski, J. V. Ortiz, A. G. Baboul, B. B. Stefanov, G. Liu, A. Liashenko, P. Piskorz, I. Komaromi, R. Gomperts, R. L. Martin, D. J. Fox, T. Keith, M. A. Al-Laham, M. A. Peng, A. Nanayakkara, C. Gonzalez, C. Challacombe, P. M. W. Gill, B. Johnson, W. Chen, M. W. Wong, J. L. Andres, C. Gonzalez, M. Head-Gordon, E. S. Replogle, and J. A. Pople, *Gaussian 98, Revision A.9* (Gaussian Inc., Pittsburgh, PA, **1998**).

